ESRF	**Experiment title:** Microvascular disease induced osteocytic matrix changes in type 2 diabetic bone	**Experiment number**: MD-1388
Beamline: ID13	**Date of experiment**: from: 20/09/2023 to: 23/09/2023	**Date of report**: 22/12/2023
Shifts: 9	**Local contact(s)**: Manfred Burghammer	*Received at ESRF:*

Names and affiliations of applicants (* indicates experimentalists):

Dr. Eva Maria Wölfel*, Molecular Endocrinology Department, University of Southern Denmark, Denmark

MSc. Sebastian Zanner*, Molecular Endocrinology Department, University of Southern Denmark, Denmark

PhD Maja Østergaard*, Interdisciplinary Nanoscience Centre, Aarhus University, Denmark

Prof. Morten Frost Nielsen*, Molecular Endocrinology Department, University of Southern Denmark, Denmark

Prof. Henrik Birkedal, Interdisciplinary Nanoscience Centre, Aarhus University, Denmark

Report:

The aim of the project is to characterise the bone matrix surrounding the osteocyte lacunae (perilacunar matrix) to determine potential differences in mineral and collagen composition in type 2 diabetic individuals with and without microvascular disease. Previous work from Zanner *et al.* [1] showed that in patients with type 2 diabetes mellitus complicated with microvascular disease the osteocyte lacunar volume in the cortical bone compartment was enlarged compared to type 2 diabetes individuals without microvascular complications. The osteocyte network, composed of osteocyte lacunae where the osteocyte residue and its canaliculi (processes connecting osteocytes and cells on the bone surface), and its surrounding matrix play a pivotal role in bone material quality. Understanding its changes due to diabetes complications enhances our knowledgeand its contribution to diabetes induced bone impairments. Thus, we set out to validate our hypothesis of differing perilacunar matrix composition changes by applying high resolution scanning XRF/XRD/SAXS on thin bone sections at ID13.

Ten iliac crest biopsies (5 per group) were cut in 4 µm thin sections using a microtome. This thickness is used in histological routine and has been shown to include isolated osteocyte lacunar surfaces while still ensuring sufficient sample quality. The sections were then carefully mounted on 5 x 5 mm silicon nitride frames using super glue.

With guidance from the beamline scientist, the frames containing the bone sections were glued to a small glass microscopy slide and a magnet was glued to the bottom of the glas slide to mount the samples on the sample stage. In addition, two frames were fitted on one piece of glass to reduce sample exchanging. The sample was mounted on a piezo stage enabling us to do fine scans while the hexapod underneath the piezo enabled for bigger movements to position the sample properly. We used a beam energy of 15.2 keV and the beam was focused down to 340 nm × 340 nm using a pair of silicon compound refractive lenses. Downstream from the sample a flighttube was placed immediately before the beam stop. The diffraction signal was collected by an Eiger 4M detector, while at an angle of app. 90 degrees towards the control hutch a Vortex-EM detector collected the

fluorescence signal. For defining the region-of-interest (ROI) of high-resolution scans, a microscope was moved in downstream of the sample instead of the flighttube, beamstop, and diffraction detector.

In total, 10 samples were measured (five samples per group, type 2 diabetes with and without microvascular disease). In pre selected regions (based on optical microscopy, see Fig 1a) an overview scan was performed with dimension of 400 µm × 400 µm and a step size of 1 µm and exposure time of 0.005 s (Fig1b). Within the overview scan, osteocyte lacunae were located and scanned with 40 µm × 40 µm map size and a step size of 250 nm and an exposure time of 0.01 s (Fig 1c-h). This process was repeated for every sample until app. 20 osteocyte lacunae were measured in per sample, to obtain statistical robustness.
During the beamtime we experienced problems with the detector and the software that was frozen, which required a restart of the Eiger 4M and the software, so it had to be restarted. In our case, the software problems were not detrimental, but a smoothly running beamtime is always preferable, both for users and the beamline scientists. We were however very satisfied with the GUI implementation that enabled us to click on the microscope image to move the sample to the point we aimed at.

Following the beamtime, we have integrated the diffraction data with MatFRAIA [2], while data processing and analysis is ongoing. Currently, we are looking at the WAXS signal, fitting selected peaks in the diffractogram and visualizing maps of these (Fig 1e-h). The obtained maps show interesting features in the peri-lacunar neighbourhood, however further analysis is required prior to conlusions. We intend to fit the XRF data in PyMCA (see expected results in Fig 1c-d). In addition, we also plan to take a closer look at the SAXS signal.

The influence of osteocytes on the diabetic bone fragility as well as the mechanism of osteocyte enlargement are still under debate and the results of the ongoing analysis are expected to have significant impact on both, the mechanisms in peri-lacunar remodelling and diabetic bone impairements. We expect the experiment to result in a publication pending the completion of the data analysis.

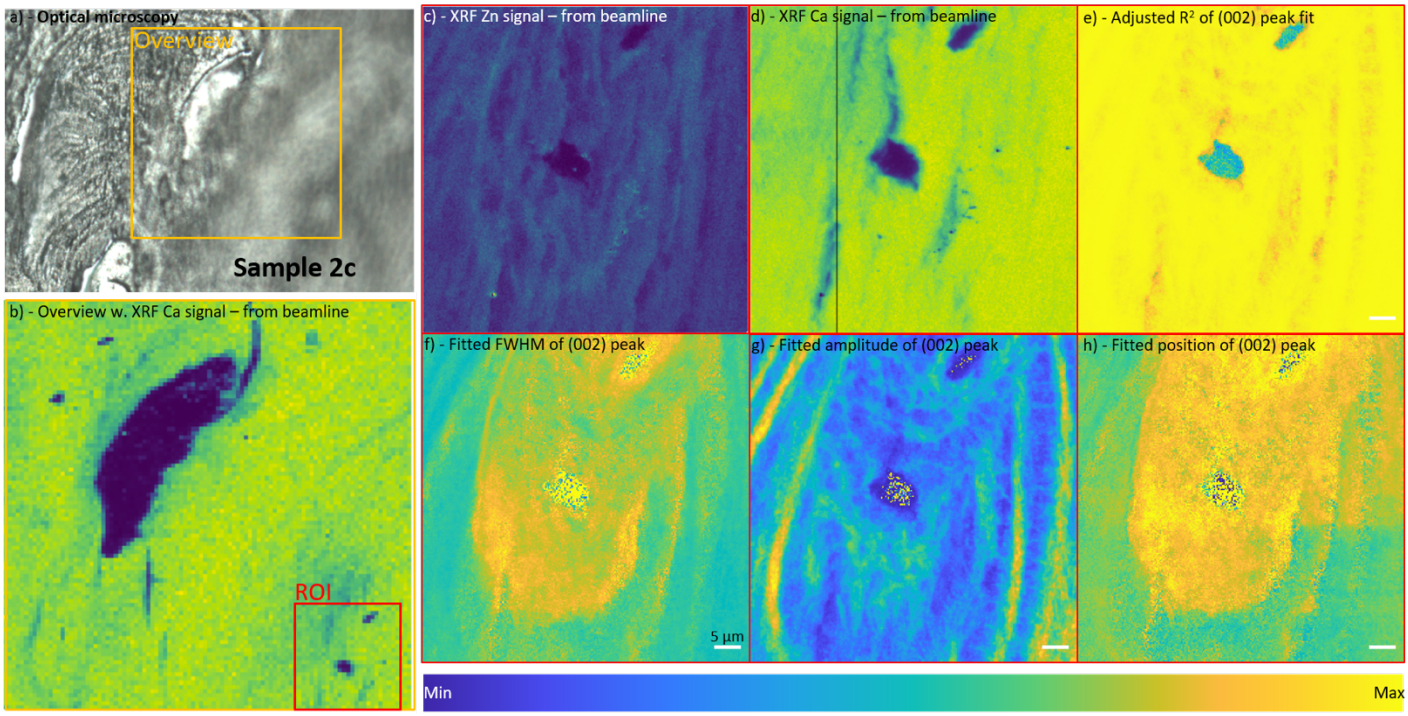

Figure 1 – Preliminary data analysis. **a)** Optical microscopy image of a region in a bone section. The area where an overview scan was performed is indicated with the orange box. **b)** The XRF Ca summed signal (screenshot from beam line) of the overview scan with red box indicating the ROI scan region. **c-d)** XRF Zn and Ca summed signal (screenshot from beam line) of the ROI scan, respectively. **e-h)** Maps from results of Lorentz fit of (002)-peak in diffractograms, depicting e) the adjusted R^2 of the fit (color bar: [0 1]), f) the peak FWHM (color bar: [0 0.25]), g) the peak amplitude (color bar: [0 1500]), and h) the peak position (color bar: [13.56° 13.61°]). All scale bars depicts 5 µm.

References:

[1] S. Zanner et al., *JBMR Plus* 7, e10832 (2023).
[2] A. Bernthz et al., *Journal of Synchrotron Radiation* 29 (6), 1420-1428 (2022).